Electrophoresis of a thin charged disk

J. D. Sherwood[a)]
Schlumberger Cambridge Research, High Cross, Madingley Road, Cambridge CB3 0EL, United Kingdom

H. A. Stone
Division of Applied Sciences, Harvard University, Cambridge, Massachusetts 02138

(Received 31 August 1994; accepted 14 December 1994)

The electrophoretic velocity of a charged disk of zero thickness is computed in the limit of small surface potentials, but with arbitrary double layer thickness. The disk represents an idealized clay particle, and has uniform surface charge over its flat surface, together with a uniform line charge around its edge. The contributions of these two charges to the electrophoretic velocity are considered separately. Asymptotic results are obtained for thin and thick double layers, and intermediate results are obtained by numerical integration. The singularities in both the electrical and hydrodynamic fields at the edge of the particle enhance the importance of the edge charge when the double layer thickness κ^{-1} is small compared to the disk radius a. © *1995 American Institute of Physics.*

I. INTRODUCTION

We consider the electrophoresis of a charged circular disk of zero thickness. The charge density σ on the surface of the particle is assumed to be uniform, as is the line charge density q around the circular edge of the disk. The disk represents an idealized plate-like clay particle (e.g., montmorillonite), with a negative surface charge σ caused by substitutions in the crystal lattice of the clay, and an edge charge q which depends upon the pH within the surrounding fluid.

Clays are widely studied because of their importance in agriculture and civil engineering, and because of their use as vicosifiers in industrial products ranging from pharmaceuticals to drilling fluids. The state of flocculation (and hence the rheology) of an aqueous suspension of clay particles depends upon the charges on the clay, and it is therefore important to be able to interpret measurements of the electrophoretic velocity of such particles. These velocities can increase[1,2] by as much as 50% as the pH increases to values above 10. We shall assume that the charge density σ of the crystal lattice is uniform over the surface of the particle. However, some studies suggest that the electrophoretic velocity is independent of electrolyte concentration, implying that a constant surface potential may be a more appropriate boundary condition. We return to this point in Sec. V.

Montmorillonite particles have a thickness typically 1 nm and lateral dimensions typically up to 1 μm. If suspended in an aqueous electrolyte, the charged particle will be surrounded by a cloud of counterions. The thickness of the cloud is $O(\kappa^{-1})$, where the Debye length $\kappa^{-1} \simeq 10$ nm in a 1–1 electrolyte of concentration 10^{-3} mol/l. Thus the Debye length is usually small compared to the lateral dimension of the particle, but is not necessarily small compared to the particle thickness. It is, therefore, not evident that Smoluchowski's result for the electrophoretic velocity of a particle with a thin double layer is valid. Here we shall study the infinitely thin disk for arbitrary values of $a\kappa$, where a is the disk radius, and investigate both surface and edge charge distributions.

Previous studies of clay-like particles have been based upon analyses of thin oblate spheroids. Yoon and Kim[3] studied spheroids with a uniform surface potential ψ_0 (rather than a uniform surface charge density σ), with arbitrary double layer thickness κ^{-1}. Fair and Anderson[4] specified the surface potential ψ_0 as a function of position over the surface of a spheroid, but assumed that the double layer was everywhere thin compared to the particle dimension. Here we shall tackle the disk geometry directly by means of Hankel transforms. We consider a uniform surface charge density σ and a uniform edge charge q, with no restriction on the Debye length κ^{-1}.

We assume that the charge cloud can be described by means of the linearized Poisson–Boltzmann equation, and we shall neglect deformation of the charge cloud caused either by the applied electric field $\mathbf{E}^{\infty}$ or by motion of the fluid. The Reynolds number for flow around such micron-size particles is sufficiently small that inertial effects may be neglected. Our analysis is, therefore, similar to that of Henry,[5] who studied electrophoresis of a uniformly charged sphere. These simplifying assumptions enable us to compute the electrophoretic velocity of a particle by means of the reciprocal theorem,[6,7] without the need to compute the details of the electrically driven fluid velocity around the particle. Nonspherical particles become tractable, and this approach has been used to study both rods[6] and spheroids.[3,8]

The boundary value problem is linear, and we may consider separately the case of an electric field $\mathbf{E}^{\infty}$ normal to the surface of the particle, which causes the particle to translate broadside on, and an electric field parallel to the plane of the

[a)]Corresponding author: Telephone: 44 1223 325363, fax: 44 1223 467004; e-mail: sherwood@cambridge.scr.slb.com

 1070-6631/95/7(4)/697/9/$6.00

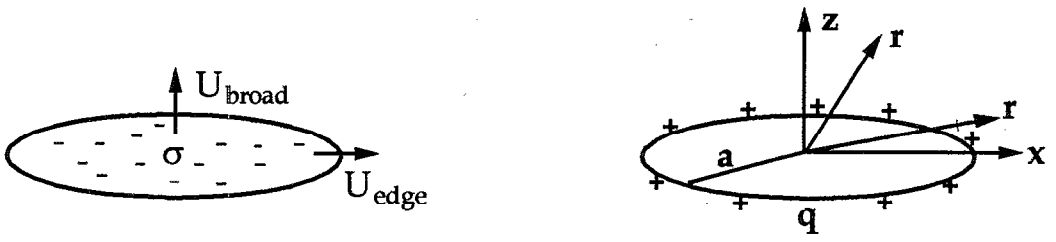

FIG. 1. Disks with uniformly distributed surface and edge charges. Application of an electric field parallel or perpendicular to the disk face produces, respectively, edgewise or broadside translation.

particle, which leads to edgewise motion. The total charge on a particle of radius a is $Q=2\pi(a^2\sigma+aq)$. If the charge cloud is very large compared to the size of the disk (i.e., $a\kappa\ll 1$), the cloud is sufficiently diffuse that it may be ignored. The electrical force $Q\mathbf{E}^{\infty}$ acting on the particle is balanced by the Stokes drag, which for a particle translating in a Newtonian fluid of viscosity μ is $16\mu a U_{\text{broad}}$ for broadside motion with velocity U_{broad}, and $(32/3)\mu a U_{\text{edge}}$ for edgewise motion with velocity U_{edge}.

When the particle is surrounded by a charge cloud of counterions, the applied electric field will act on the ions, thereby creating a body force which causes motion of the fluid. This fluid motion will act on the particle, and will reduce the electrophoretic velocity. The basic governing equations for electrokinetic phenomena are available in standard references (e.g., Saville[9]), and in the following sections we summarize these analyses. Our work is based on (previously published) solutions of the Laplace equation, the linearized Poisson–Boltzmann equation and the Stokes equations, obtained by means of Hankel transforms and summarized in Sec. II, and we deal directly with the disk geometry with its sharp edges rather than studying the limiting case of an analysis for (smooth) oblate spheroids. Analytical estimates for the translational speed for edge and surface charge distributions are determined in Sec. III, for the thin ($a\kappa\gg 1$) and thick ($a\kappa\ll 1$) double layer limits. Numerical results for $10^{-1}<a\kappa<10^{2}$ are given in Sec. IV and are compared with the asymptotic analyses. A discussion of the applicability of this work to real clays is provided in Sec. V.

II. ANALYSIS

A. Equilibrium charge cloud

We suppose that the disk, of radius a, is suspended in a Newtonian electrolyte of viscosity μ, containing m species of ions, with valence z_i $(i=1,\ldots,m)$ and number density $n^i(\mathbf{r})$, where $\mathbf{r}$ denotes position (see Fig. 1). Far away from the surface of the charged disk, the ionic number densities attain bulk values n^i_{∞}. In the absence of any applied field or fluid motion, the ionic densities satisfy the Boltzmann distribution

$$n^i_0=n^i_{\infty}\exp(-ez_i\phi_0/kT), \tag{1}$$

where e is the electronic charge, k is Boltzmann's constant, and T is the temperature. The electric potential ϕ_0 satisfies the Poisson equation

$$\nabla^2\phi_0=-\sum_{i=1}^{m}\frac{ez_in^i_0}{\epsilon}, \tag{2}$$

where ϵ is the permittivity of the electrolyte. We shall assume that the potentials are small (i.e., $e\phi_0/kT\ll 1$) so that we may linearize the Poisson–Boltzmann equation obtained by combining (1) and (2). This linearization leads to

$$\nabla^2\phi_0=\kappa^2\phi_0, \tag{3}$$

where the Debye length κ^{-1}, which characterizes the thickness of the charge cloud, is defined by

$$\kappa^2=\sum_{i=1}^{m}\frac{e^2z_i^2n^i_{\infty}}{\epsilon kT}. \tag{4}$$

The local ion charge density $\rho=\sum_{i=1}^{m}ez_in^i$ becomes, in the limit $e\phi_0/kT\ll 1$,

$$\rho_0(\mathbf{r})=-\epsilon\kappa^2\phi_0(\mathbf{r}). \tag{5}$$

For the case of a disk with uniform surface charge density σ, the potential ϕ_0 in the upper half-plane $z\geqslant 0$ satisfies the boundary conditions

$$\epsilon\frac{\partial\phi_0}{\partial z}=-\sigma, \quad z=0^+, \quad 0\leqslant r<a, \tag{6a}$$

$$\epsilon\frac{\partial\phi_0}{\partial z}=0, \quad z=0, \quad r>a, \tag{6b}$$

$$\phi_0\to 0, \quad |\mathbf{r}|\to\infty. \tag{6c}$$

The solution to the linear Poisson–Boltzmann equation (3) satisfying the boundary conditions (6a)–(6c), may be obtained by means of Hankel transforms:

$$\phi_0(r,z)=\frac{\sigma a}{\epsilon}\int_0^{\infty}\frac{J_1(at)J_0(rt)}{(\kappa^2+t^2)^{1/2}}\exp[-(\kappa^2+t^2)^{1/2}z]\,dt$$

$$=\frac{Q_{\text{surf}}}{2\pi a\epsilon}\bar{\phi}_0(r,z), \tag{7}$$

where the J_i are Bessel functions and Q_{surf} is the total surface charge on the disk; (7) defines the function $\bar{\phi}_0$. If $a\kappa\gg 1$, and $z\ll a$, the potential will be that above an unbounded, charged plane

$$\phi_0(r,z)=\sigma\exp(-\kappa z)/\epsilon\kappa \tag{8}$$

in the region $a-r\gg\kappa^{-1}$ away from the edge of the disk.

For the case of a uniform edge (or ring) charge with line density q, the boundary conditions (6a)–(6b) must be replaced by

$$\epsilon \frac{\partial \phi_0}{\partial z} = -\frac{1}{2} q \delta(r-a) \quad z=0^+, \tag{9}$$

and this leads to the potential

$$\phi_0(r,z) = \frac{qa}{2\epsilon} \int_0^\infty \frac{tJ_0(at)J_0(rt)}{(\kappa^2+t^2)^{1/2}} \exp[-(\kappa^2+t^2)^{1/2}z]dt$$

$$= \frac{Q_{\text{edge}}}{4\pi a \epsilon} \bar{\phi}_0(r,z). \tag{10}$$

Note that the potential will become large close to a line charge, with a logarithmic singularity. In practice, if the line charge density q is too high, counterion condensation can occur.[10,11] The limiting line charge density $q \simeq 4\pi\epsilon kT/e$, corresponds to a line of isolated charges e separated by 0.7 nm in water at 25 °C, and we assume that the line charge q around the disk is sufficiently low to avoid condensation.

We draw the reader's attention to finite element solutions of the nonlinear Poisson–Boltzmann equation around a charged disk of finite thickness, obtained by Secor and Radke[12] and Chang and Sposito.[13]

B. The perturbed charge cloud

When an electric field $\mathbf{E}^\infty$ is applied, the charge cloud around the particle will be perturbed, both by the direct electrical forces acting on the ions, and by the motion of the fluid. Ions are convected with the fluid velocity $\mathbf{u}$, and move relative to the fluid under the influence of electric fields and thermal diffusion, and hence the conservation equation for the ith ionic species, in steady state, is

$$\nabla \cdot [n^i \mathbf{u} - \omega^i (kT \nabla n^i + e z_i n^i \nabla \phi)] = 0, \tag{11}$$

where ω^i denotes the mobility of the ith species.

We follow Saville[9] and nondimensionalize potentials by kT/e, lengths by a, velocities by $\epsilon(kT/e)^2/\mu a$, and mobilities by ω^0. We assume that the potential aE^∞ which characterizes the applied field is small compared to the equilibrium zeta potential ψ_0 at the surface of the particle, so that $\beta = aeE^\infty/kT \ll e\psi_0/kT$, where $e\psi_0/kT$ has already been assumed small in order to derive the linearized Poisson–Boltzmann equation (3). We use the dimensionless field strength β as the basis for a perturbation expansion:

$$\hat{\mathbf{u}} = \beta \hat{\mathbf{u}}_1 + \cdots, \tag{12a}$$

$$\hat{\phi} = \hat{\phi}_0 + \beta \hat{\phi}_1 + \cdots, \tag{12b}$$

$$n^i = n_0^i + \beta n_1^i + \cdots, \tag{12c}$$

where the subscript 0 refers to the equilibrium cloud, and the caret $\hat{}$ denotes a nondimensional quantity. The steady-state ion conservation equation, correct to $O(\beta)$ becomes

$$P_e \hat{\mathbf{u}}_1 \cdot \nabla n_0^i = \hat{\omega}^i \nabla \cdot (z_i n_0^i \nabla \hat{\phi}_1 + z_i n_1^i \nabla \hat{\phi}_0 + \nabla n_1^i), \tag{13}$$

where the Péclet number $P_e = \epsilon kT/e^2 \mu \omega^0$ is a measure of the ratio of ionic convection to diffusion. Since the nondimensional equilibrium potential $\hat{\phi}_0$ has been assumed to be small, (13) reduces to

$$0 = z_i n_\infty^i \nabla^2 \hat{\phi}_1 + \nabla^2 n_1^i. \tag{14}$$

The (dimensional) boundary conditions at infinity are

$$n_1^i \to 0, \tag{15a}$$

$$\beta \phi_1 \sim -\mathbf{E}^\infty \cdot \mathbf{r}. \tag{15b}$$

We assume that no ions enter or leave the surface of the particle. Hence

$$\mathbf{n} \cdot (kT \nabla n^i + e z_i n^i \nabla \phi) = 0, \tag{16}$$

where $\mathbf{n}$ is the normal to the particle surface. At $O(\beta)$, and assuming $\hat{\phi}_0 \ll 1$, this zero flux boundary condition becomes

$$\mathbf{n} \cdot \nabla (n_1^i + z_i n_\infty^i \hat{\phi}_1) = 0. \tag{17}$$

Multiplying Eq. (14) by $e^2 z_i$ and summing over i, we obtain, at $O(\beta)$

$$\nabla^2 \hat{\chi}_1 = 0, \tag{18}$$

where

$$\hat{\chi}_1 = \hat{\phi}_1 + \hat{\rho}_1 (a\kappa)^{-2} \tag{19}$$

and

$$\hat{\rho}_1 = \frac{ea^2 \rho_1}{\epsilon kT} = \frac{ea^2}{\epsilon kT} \sum_{i=1}^m e z_i n_1^i \tag{20}$$

is the (nondimensional) perturbation to the charge density ρ. The boundary conditions for (18) are obtained in similar fashion from Eqs. (15) and (17):

$$\hat{\chi}_1 \sim -\hat{\mathbf{E}} \cdot \hat{\mathbf{r}} \quad \text{as } \mathbf{r} \to \infty, \tag{21a}$$

$$\mathbf{n} \cdot \nabla \hat{\chi}_1 = 0 \quad \text{on the particle surface}, \tag{21b}$$

where $\hat{\mathbf{E}}$ is a unit vector in the direction of the applied field $\mathbf{E}^\infty$. The (dimensional) potential

$$\chi = \phi_1 + \rho_1/\epsilon\kappa^2 \tag{22}$$

is thus obtained by solving Laplace's equation for the potential around an insulating particle in a uniform field.

The solution of Laplace's equation for the potential around a disk is straightforward if the applied field $\mathbf{E}^\infty$ is parallel to the surface of the disk, since an infinitesimally thin disk does not perturb the electric field. Hence

$$\chi(r,z) = -\mathbf{E}^\infty \cdot \mathbf{r} \quad \text{(edgewise motion)}. \tag{23}$$

If the applied field $\mathbf{E}^\infty$ is normal to the surface of the disk, the field may be obtained by means of Hankel transforms,[14] and is

$$\chi(r,z) = -E^\infty z - \frac{2E^\infty}{\pi} \int_0^\infty [t^{-2} \sin(at) - at^{-1} \cos(at)]$$

$$\times \exp(-tz) J_0(rt) dt, \quad z \geq 0. \tag{24}$$

Integrating by parts, scaling all lengths by a, making the transformations (a conversion to oblate spheroidal coordinates)

$$z=\lambda\zeta, \quad r^2=(1+\lambda^2)(1-\zeta^2) \quad (0\leqslant\zeta\leqslant 1, \ 0\leqslant\lambda<\infty) \tag{25}$$

and using Sec. 6.752 of Gradshteyn and Ryzhik,[15] we obtain

$$\chi(r,z)=-E^\infty z+\frac{2E^\infty}{\pi}(z\cot^{-1}\lambda-\zeta)(\text{broadside motion}). \tag{26}$$

We shall later require

$$\frac{\partial\chi}{\partial z}=-E^\infty+\frac{2E^\infty}{\pi}\int_0^\infty[t^{-1}\sin t-\cos t]\times\exp(-tz)J_0(rt)dt$$
$$=-E^\infty+\frac{2E^\infty}{\pi}\left(\cot^{-1}\lambda-\frac{\lambda}{\lambda^2+\zeta^2}\right), \tag{27a}$$

$$\frac{\partial\chi}{\partial r}=\frac{2E^\infty}{\pi}\int_0^\infty[t^{-1}\sin t-\cos t]\exp(-tz)J_1(rt)dt$$
$$=\frac{2E^\infty}{\pi}\frac{\zeta(1-\zeta^2)}{r(\lambda^2+\zeta^2)}. \tag{27b}$$

C. Fluid motion and an application of the reciprocal theorem

The Stokes equations are modified by the presence of an electric force $\rho\mathbf{E}$ acting on the fluid. Expanding in powers of β, we obtain

$$\rho\nabla\phi=(\rho_0+\beta\rho_1)\nabla(\phi_0+\beta\phi_1)+O(\beta^2)$$
$$=-\nabla(\tfrac{1}{2}\epsilon\kappa^2\phi_0^2-\beta\rho_1\phi_0)+\beta\rho_0\nabla(\phi_1+\rho_1/\epsilon\kappa^2)+O(\beta^2), \tag{28}$$

where we have made use of the identity $\rho_0=-\epsilon\kappa^2\phi_0$. Hence the Stokes equations become

$$\mu\nabla^2\mathbf{u}-\nabla p-\rho_0\nabla\chi=0, \tag{29}$$

where the term $\nabla(\frac{1}{2}\epsilon\kappa^2\phi_0^2-\beta\rho_1\phi_0)$ in (28) has been incorporated into the pressure p. The effect of this additional pressure on the particle is canceled by terms in the direct electric stress (33) discussed below.

The force on the particle may now be evaluated by means of the reciprocal theorem for Stokes flows.[16] Details are given by Sherwood[6] and by Teubner.[7] If the (uncharged) particle translates with velocity $\mathbf{U}$, it exerts a force $\mathbf{F}_{\text{Stokes}}=\mathbf{R}\cdot\mathbf{U}$ on the fluid where $\mathbf{R}$ is the resistance tensor for the particle. The corresponding fluid velocity is

$$\mathbf{u}(\mathbf{r})=\mathbf{G}(\mathbf{r})\cdot\mathbf{U}, \tag{30}$$

where $\mathbf{G}(\mathbf{r})$ is a second rank tensor, with $\mathbf{G}=\mathbf{I}$ (the identity tensor) on the surface of the particle. The velocity far from the particle will be that due to a Stokeslet of strength $\mathbf{F}_{\text{Stokes}}$, and hence, for $|\mathbf{r}|\gg a$,

$$\mathbf{G}(\mathbf{r})\sim\mathbf{J}(\mathbf{r})\mathbf{R},$$

where

$$\mathbf{J}(\mathbf{r})=\frac{1}{8\pi\mu r}\left(\mathbf{I}+\frac{\mathbf{rr}}{r^2}\right), \tag{31}$$

and $\mathbf{r}$ is the position vector relative to the center of the particle.

The effect of the electric body force per unit volume, $-\rho_0\nabla\chi$, in the Stokes equation (29) will create a disturbance flow in the fluid surrounding the particle, which results in a force on the particle

$$\mathbf{F}_{\text{cloud}}=-\int_V\rho_0\nabla\chi\cdot\mathbf{G}\,dV, \tag{32}$$

where the volume integral extends over the entire fluid volume V outside the particle.

The electric force $\mathbf{F}_e$ acting directly on the particle may be obtained by integrating the Maxwell stress tensor $\mathbf{m}$ over the surface S of the particle, to obtain[7]

$$\mathbf{F}_e=\int_S\mathbf{m}\cdot\mathbf{n}\,dS=\int_V\rho\nabla\phi\,dV, \tag{33}$$

where $\mathbf{n}$ is the outward normal to the surface of the particle and V is again the entire fluid volume outside the particle. The equilibrium contribution $\rho_0\nabla\phi_0$ is balanced by the pressure acting over the surface of the particle, and as in the Stokes equation (29), the leading-order contribution to the direct electric force may be expressed as

$$\mathbf{F}_e=\int_V\rho_0\nabla\chi\,dV. \tag{34}$$

If the charge cloud is large compared to the size of the particle, we may approximate $\nabla\chi$ as $-\mathbf{E}^\infty$, and hence $\mathbf{F}_e\simeq Q\mathbf{E}^\infty$; this simplification was used by Sherwood.[6] Combining the fluid stress (32) and the direct electric force (34), the total force balance on the particle may be written as

$$\int_V\rho_0\nabla\chi\cdot(\mathbf{I}-\mathbf{G})dV-\mathbf{R}\cdot\mathbf{U}=0. \tag{35}$$

Note that the fluid motion caused by direct electrical forces acting on the fluid, and that caused by motion of the particle, will create additional deformation of the charge cloud, but, as seen from Eq. (13), this deformation will be $O(\hat{u}_1 P_e\hat{\phi}_0)$, and may be neglected when the potential $\hat{\phi}_0$ is small.

Equation (35) gives the electrophoretic translation velocity of an arbitrarily shaped particle accounting for the influence of the charge cloud. Knowledge of $\mathbf{G}$ and $\mathbf{R}$ for a given particle shape, along with the corresponding solutions for χ and ϕ_0, allow calculation of $\mathbf{U}$. We now turn the explicit form of $\mathbf{G}$ for disk-shaped particles.

Several authors have studied Stokes flow around a disk: Ray[17] and Gupta[18] considered the case of broadside motion and Ray[17] and Davis[19] considered the case of edgewise motion; results are conveniently summarized by Tanzosh.[20] The components of the tensor $\mathbf{G}$ (for $z\geqslant 0$) that we require, expressed in the spheroidal coordinates (λ,ζ), are

$$G_{rz}=\frac{2}{\pi}\int_0^\infty z\sin tJ_1(rt)\exp(-tz)dt=\frac{2}{\pi}\frac{z\lambda(1-\zeta^2)}{r(\lambda^2+\zeta^2)}, \tag{36a}$$

$$G_{zz}=\frac{2}{\pi}\int_0^\infty (1+tz)\,\frac{\sin t}{t}J_0(rt)\exp(-tz)dt$$

$$=\frac{2}{\pi}\left(\cot^{-1}\lambda+\frac{\lambda\zeta^2}{\lambda^2+\zeta^2}\right), \tag{36b}$$

$$G_{xx}=\frac{2}{3\pi}\int_0^\infty \frac{\sin t}{t}\exp(-tz)[(1+tz)J_2(rt)\cos 2\theta$$

$$+(3-tz)J_0(rt)]dt$$

$$=\frac{2}{3\pi}\left(\frac{\lambda^2(1-\zeta^2)}{(1-\lambda^2)(\lambda^2+\zeta^2)}\cos 2\theta+3\cot^{-1}\lambda-\frac{\lambda\zeta^2}{\lambda^2+\zeta^2}\right)$$

$$\equiv G_{xx}^{(1)}\cos 2\theta+G_{xx}^{(2)}. \tag{36c}$$

The well-known resistance coefficients characterizing disk translation in a Stokes flow are (e.g., Happel and Brenner[16])

$$R_{xx}=\frac{32}{3}\mu a,\quad R_{zz}=16\mu a. \tag{37}$$

Substituting $\mathbf{G}$ (36), ρ_0 (5), and $\nabla\chi$ (27) into the force balance (35), performing the angular integration, and scaling lengths by a and χ by aE^∞, the electrophoretic velocity of a disk in an electric field normal to the plane of the disk is (broadside motion)

$$U_{\text{broad}}=\frac{QE^\infty(a\kappa)^2}{8\mu a}\int_{r=0}^\infty\int_{z=0}^\infty \tilde{\phi}_0\left(\frac{\partial\chi}{\partial z}(G_{zz}-1)\right.$$

$$\left.+\frac{\partial\chi}{\partial r}G_{rz}\right)r\,dr\,dz. \tag{38}$$

If the electric field is parallel to the face of the disk, we obtain the edgewise translational velocity

$$U_{\text{edge}}=\frac{3QE^\infty(a\kappa)^2}{16\pi\mu a}\int_{r=0}^\infty\int_{z=0}^\infty \tilde{\phi}_0(1-G_{xx}^{(2)})r\,dr\,dz, \tag{39a}$$

$$=\frac{3QE^\infty}{32\mu a}\left(1-2(a\kappa)^2\int_{r=0}^\infty\int_{z=0}^\infty \tilde{\phi}_0 G_{xx}^{(2)}r\,dr\,dz\right), \tag{39b}$$

where

$$G_{xx}^{(2)}=\frac{2}{3\pi}\int_0^\infty\left(\frac{3}{t}-z\right)\sin t\,\exp(-tz)J_0(rt)dt$$

$$=\frac{2}{3\pi}\left(3\cot^{-1}\lambda-\frac{\lambda\zeta^2}{(\lambda^2+\zeta^2)}\right). \tag{40}$$

For arbitrary values of $a\kappa$ we must evaluate these expressions numerically. However, for the limiting cases of thin and thick double layers, it is possible to obtain analytical estimates, as shown in the next section.

III. ASYMPTOTIC RESULTS FOR $a\kappa\gg1$ AND $a\kappa\ll1$

A. Thin double layers—Edgewise motion with a uniform surface charge

When the disk is uniformly charged and the double layer thin, $\kappa a\gg1$, we may approximate the equilibrium potential by (8), except over a negligibly small region at the edge of the disk, and the integration in (39) need only be taken over the region $0\leqslant r\leqslant1$. Performing first the integration over z, and then the integration over r, we obtain

$$\int_{r=0}^1\int_{z=0}^\infty \tilde{\phi}_0 G_{xx}^{(2)}r\,dr\,dz$$

$$=\frac{2}{3\pi a\kappa}\int_{r=0}^1\int_{t=0}^\infty \frac{\sin t}{t}\frac{(2t+3a\kappa)}{(t+a\kappa)^2}J_0(rt)r\,dr\,dt$$

$$=\frac{2}{3\pi a\kappa}\int_{t=0}^\infty \frac{\sin t}{t^2}\frac{(2t+3a\kappa)}{(t+a\kappa)^2}J_1(t)dt$$

$$=\frac{1}{2(a\kappa)^2}-\frac{8}{3\pi(a\kappa)^3}+O(a\kappa)^{-4}, \tag{41}$$

where we have used the results[21]

$$\int_0^\infty \frac{\sin t}{t^2}J_1(t)dt=\frac{\pi}{4},\quad \int_0^\infty \frac{\sin t}{t}J_1(t)dt=1. \tag{42}$$

Hence, to leading order when $a\kappa\gg1$,

$$U_{\text{edge}}=\frac{Q_{\text{surf}}E^\infty}{2\mu\pi a^2\kappa}=\frac{\psi_0\epsilon E^\infty}{\mu} \tag{43}$$

which is Smoluchowski's result; note that we have used the fact that a uniformly charged surface in the thin double layer limit may be characterized by a uniform zeta potential $\psi_0=\sigma/\kappa\epsilon=Q_{\text{surf}}/2\pi a^2\kappa\epsilon$.

The results of the next section (III B) suggest that edge corrections to (43) will be $O(a\kappa)^{-1/2}$ smaller.

B. Thin double layers—Edgewise motion with a uniform edge charge

We next consider the limit $a\kappa\gg1$ for the edgewise motion of a disk with an edge charge. The dominant contribution to the integral comes from the vicinity of the edge and so we carefully consider the neighborhood of $(r,z)=(1,0)$ where the spheroidal coordinates (ζ,λ) are small, i.e., $\zeta\ll1$, $\lambda\ll1$. Using a local system of cylindrical coordinates (R,α) based on the edge of the disk, with the angle $\alpha=0$ corresponding to the plane $z=0$ outside the surface of the disk, we find

$$R\cos\alpha=r-1\simeq\tfrac{1}{2}(\lambda^2-\zeta^2), \tag{44a}$$

$$R=[(r-1)^2+z^2]^{1/2}\simeq\tfrac{1}{2}(\lambda^2+\zeta^2), \tag{44b}$$

and hence

$$\lambda^2\simeq R(1+\cos\alpha)=2R\cos^2(\alpha/2), \tag{45a}$$

$$\zeta^2\simeq R(1-\cos\alpha)=2R\sin^2(\alpha/2). \tag{45b}$$

The dominant contribution to $G_{xx}^{(2)}$ in the neighborhood of the edge is

$$G_{xx}^{(2)}=\frac{2}{3\pi}\left(3\cot^{-1}\lambda-\frac{\lambda\zeta^2}{\lambda^2+\zeta^2}\right)$$
$$=\frac{2}{3\pi}\left(\frac{3\pi}{2}-3\lambda+\cdots-\frac{\lambda\zeta^2}{\lambda^2+\zeta^2}\right)$$
$$=1-\frac{2}{3\pi}(2R)^{1/2}\cos\left(\frac{\alpha}{2}\right)\left[3+\sin^2\left(\frac{\alpha}{2}\right)\right]+\cdots. \quad (46)$$

If $a\kappa\gg1$, we may neglect curvature of the edge charge. The potential around the edge charge of density $q=Q_{\text{edge}}/2\pi a$ may be approximated by that around an infinite line charge:

$$\phi_0=\frac{q}{2\pi\epsilon}K_0(a\kappa R), \quad (47)$$

where K_0 is a modified Bessel function and R has been nondimensionalized by the disk radius a; the corresponding charge density follows from (5).

An electric field applied parallel to the surface of the disk is not perturbed by the disk, so $\nabla\chi=-\mathbf{E}^\infty$. Inserting these asymptotes (46), (47) into the force balance (35) we obtain

$$\frac{32\mu aU_{\text{edge}}}{3}=2\pi a^3\int_0^\infty R\,dR\int_{-\pi}^{\pi}d\alpha\,\frac{\kappa^2 q}{2\pi}$$
$$\times K_0(a\kappa R)E^\infty\frac{2}{3\pi}(2R)^{1/2}$$
$$\times\cos\left(\frac{\alpha}{2}\right)\left[3+\sin^2\left(\frac{\alpha}{2}\right)\right]. \quad (48)$$

Integrating first with respect to the angle α gives

$$\frac{32\mu aU_{\text{edge}}}{3}=\frac{80\sqrt{2}}{9\pi}a^3\kappa^2qE^\infty\int_0^\infty R^{3/2}K_0(a\kappa R)dR. \quad (49)$$

This integral may be evaluated analytically using the result (Watson,[21] p. 388)

$$\int_0^\infty y^{\mu-1}K_\nu(y)dy=2^{\mu-2}\Gamma\left(\frac{\mu-\nu}{2}\right)\Gamma\left(\frac{\mu+\nu}{2}\right). \quad (50)$$

Hence the electrophoretic velocity in the limit $a\kappa\gg1$ is

$$U_{\text{edge}}=\frac{3Q_{\text{edge}}E^\infty}{32\mu a}\frac{80[\Gamma(\frac{5}{4})]^2}{9\pi^2(a\kappa)^{1/2}}, \quad (51)$$

where $\Gamma(5/4)\approx0.9064$. Comparing (43) and (51) we observe that for edgewise motion with an edge charge distribution the electrophoretic translation speed is higher than for a surface charge distribution. The electrical forces acting on the charge cloud (with total charge $-Q$) tend to oppose the motion of the particle. These forces are transmitted, via fluid stresses, to the surface of the particle, and this coupling is weaker at the edge of the disk than over the interior.

If the disk is uniformly charged, as in Sec. III A, the amount of charge within a distance $O(\kappa^{-1})$ of the edge of the disk is $O(Q_{\text{surf}}/a\kappa)$, and this, by (51), will create an electrophoretic velocity $O[Q_{\text{surf}}E^\infty/\mu a(a\kappa)^{3/2}]$. Hence edge corrections to (43) will be $O(a\kappa)^{-1/2}$ smaller.

C. Thin double layers—Broadside motion with an edge charge

For the limit $a\kappa\gg1$, the third case to consider is the broadside motion of the disk with an edge charge distribution. We proceed in a manner similar to the calculations presented above. In particular, we find that in the neighborhood of the corner

$$\frac{\partial\chi}{\partial z}=-E^\infty+\frac{2E^\infty}{\pi}\left(\cot^{-1}\lambda-\frac{\lambda}{\lambda^2+\zeta^2}\right)$$
$$=-\frac{2E^\infty}{\pi}\left(\lambda+\cdots+\frac{\lambda}{\lambda^2+\zeta^2}\right)\approx-\frac{2E^\infty}{\pi}\frac{\cos(\alpha/2)}{(2R)^{1/2}} \quad (52)$$

and

$$\frac{\partial\chi}{\partial r}=\frac{2E^\infty}{\pi}\frac{\zeta(1-\zeta^2)}{r(\lambda^2+\zeta^2)}\approx\frac{2E^\infty}{\pi}\frac{\sin(\alpha/2)}{(2R)^{1/2}}. \quad (53)$$

The hydrodynamic coupling tensor has components

$$G_{zz}=\frac{2}{\pi}\left(\cot^{-1}\lambda+\frac{\lambda\zeta^2}{\lambda^2+\zeta^2}\right)$$
$$\approx1-\frac{2}{\pi}\left(\lambda-\frac{\lambda\zeta^2}{\lambda^2+\zeta^2}\right)$$
$$\approx1-\frac{2}{\pi}(2R)^{1/2}\cos^3\left(\frac{\alpha}{2}\right) \quad (54)$$

and

$$G_{rz}=\frac{2z\lambda(1-\zeta)^2}{\pi r(\lambda^2+\zeta^2)}\approx\frac{2}{\pi}(2R)^{1/2}\cos^2\left(\frac{\alpha}{2}\right)\sin\left(\frac{\alpha}{2}\right). \quad (55)$$

The broadside electrophoretic velocity U_{broad} is given by the force balance (35)

$$16\pi\mu aU_{\text{broad}}$$
$$=2\pi a^3\int_0^\infty R\,dR\int_{-\pi}^{\pi}d\alpha\,\frac{\kappa^2q}{2\pi}K_0(a\kappa R)\frac{4E^\infty}{\pi^2}\cos^2\left(\frac{\alpha}{2}\right) \quad (56a)$$
$$=\frac{2}{\pi}(a\kappa)^2Q_{\text{edge}}E^\infty\int_0^\infty K_0(a\kappa R)R\,dR, \quad (56b)$$

and so using (50) we arrive at

$$U_{\text{broad}}=\frac{Q_{\text{edge}}E^\infty}{8\pi^2\mu a}, \quad (57)$$

which is independent of $a\kappa$.

Note that we do not present any asymptotic approximations for the broadside motion of a uniformly charged disk. The standard thin double layer analysis for the interior of the disk will lead to Smoluchowski's result (43). The edge correction will correspond roughly to (57), with an edge charge of order $Q_{\text{edge}}\sim Q_{\text{surf}}/a\kappa$, and thus cannot be neglected. Hence we expect $U_{\text{broad}}\sim CQ_{\text{surf}}E^\infty/2\mu\pi a^2\kappa$, with some unknown numerical factor C.

D. Thick double layers

If the Debye length κ^{-1} is large compared to the particle dimension a, the dominant contribution to the volume integral in (35) comes from the $O(\kappa^{-3})$ volume of the charge cloud. On this length scale the particle acts as a point charge, for which the potential of the surrounding equilibrium charge cloud is

$$\phi_0=\frac{Q\ \exp(-\kappa r)}{4\pi\epsilon r} \quad (r=|\mathbf{r}|) \tag{58}$$

and acts as a point Stokeslet, so that the tensor $\mathbf{G}$ is given by (31). The solution of the Laplace equation (18), (21) for the field around an insulating particle consists of the imposed applied field $-\mathbf{E}^{\infty}$ together with dipole and higher multipole corrections, which we can neglect as we are only interested in the dominant contribution to the integral. Inserting these approximations into the force balance (35), we obtain, for broadside motion

$$U_{\text{broad}}=\frac{QE^{\infty}}{16\mu a}\left(1-\frac{8a\kappa}{3\pi}+O(a\kappa)^2\right), \quad a\kappa\ll 1 \tag{59}$$

and for edgewise motion

$$U_{\text{edge}}=\frac{3QE^{\infty}}{32\mu a}\left(1-\frac{16a\kappa}{9\pi}+O(a\kappa)^2\right), \quad a\kappa\ll 1. \tag{60}$$

It is straightforward to apply this thick double layer analysis to the case of a disk with a uniform surface *potential* (rather than a uniform charge density). Far from the particle, the potential will still have the form (58); only the quadrupole and higher multipole terms in the expansion of the potential around a disk at uniform potential will differ from those around a disk with a uniform surface charge density. The total charge on a disk at potential ψ_0 is[22,23]

$$Q=8\epsilon a\psi_0\left[1+\frac{2}{\pi}a\kappa+\left(\frac{4}{\pi^2}-\frac{1}{3}\right)(a\kappa)^2+\cdots\right], \quad a\kappa\ll 1. \tag{61}$$

Hence at constant potential

$$U_{\text{broad}}=\frac{\epsilon\psi_0 E^{\infty}}{2\mu}\left(1-\frac{2a\kappa}{3\pi}+O(a\kappa)^2\right), \quad a\kappa\ll 1 \tag{62}$$

and

$$U_{\text{edge}}=\frac{3\epsilon\psi_0 E^{\infty}}{4\mu}\left(1+\frac{2a\kappa}{9\pi}+O(a\kappa)^2\right), \quad a\kappa\ll 1. \tag{63}$$

The above asymptotic results for $a\kappa\gg 1$ and $a\kappa\ll 1$ provide useful checks on the numerical evaluation of the electrophoretic velocity reported in the next section.

IV. NUMERICAL RESULTS

The electrophoretic velocities for broadside and edge translation were determined by numerically evaluating Eqs. (38) and (39), respectively. A rectangular grid, centered on the disk, subdivided the rz plane. The two-dimensional integration over each rectangular element was performed using the IMSL routine DQAND(), which utilizes an iterated application of Gaussian quadrature formulas; typically an absolute accuracy of 10^{-8} was specified for each integration. The evaluation of several of the intermediate integrals in the kernel [e.g., (27)] in terms of the spheroidal coordinates (λ,ζ), which are easily evaluated in terms of (r,z), greatly simplified the numerical work. The integration in the rz plane was terminated at distances large compared to $(a\kappa)^{-1}$; integration over a larger distances was performed and results reported here are accurate to within a few percent. The equilibrium potential $\bar{\phi}_0$ requires an infinite integration with an oscillatory kernel involving a product of Bessel functions and the routines described and implemented by Lucas[24] were used to calculate these integrals to an absolute accuracy of 10^{-8}.

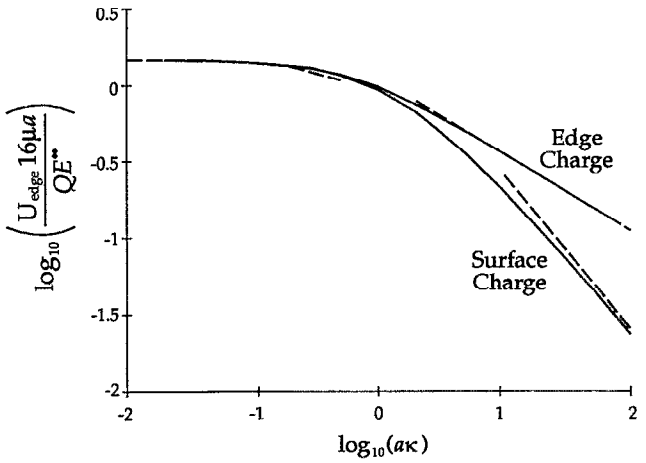

FIG. 2. The nondimensional electrophoretic velocity for edgewise translation, $U_{\text{edge}}16\mu a/QE^{\infty}$, as a function of $a\kappa$. Solid curves are the numerical results for a uniform surface charge and a uniform edge charge. Dashed curves are the asymptotic approximations (43),(51),(60) derived in Sec. III.

The computations for thin double layers ($a\kappa\gg 1$) are difficult numerically. In this limit, the gradients of the potential $\bar{\phi}_0$ are typically large near the edge of the disk; a mesh finer than $(a\kappa)^{-1}$ was set up in the neighborhood of $(r,z)=(1,0)$ in order to resolve these significant contributions to the integrals.

In Fig. 2 we show results for the electrophoretic velocity, scaled by $QE^{\infty}/16\mu a$, for edgewise translation. Both the case of a uniform surface charge and a uniform edge charge are shown with solid curves. The dashed curves are the asymptotic results described in Sec. III for both the thick (60) and thin (43), (51) double layer limits. For $a\kappa<0.1$, $a\kappa>5$ (edge charge), and $a\kappa>50$ (surface charge), the numerical results are within about ten percent of the analytical predictions. For $a\kappa<1$, where the charge cloud begins to get larger than the disk, the translation speed is the same for surface and edge charges of the same magnitude. Also, for the same double layer thickness (with $a\kappa>1$) and total charge on the disk, the disk with surface-distributed charge translates more slowly than the disk with edge-distributed charge.

In Fig. 3 we consider the case of broadside electrophoretic motion, with velocity again scaled by $QE^{\infty}/16\mu a$, for both a surface charge distribution and an edge charge distribution. Dashed curves indicate asymptotic approxima-

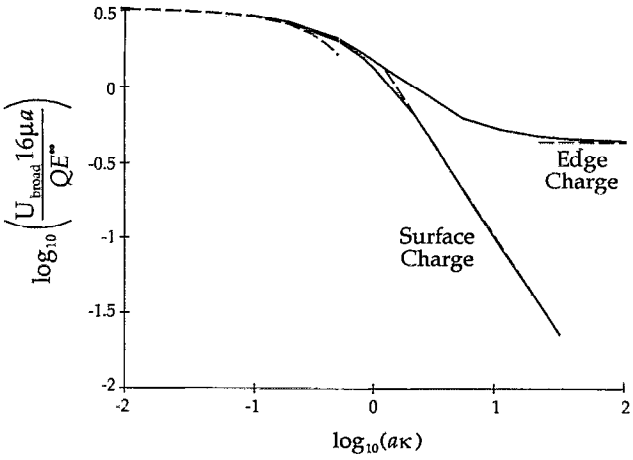

FIG. 3. The nondimensional electrophoretic velocity for broadside translation, $U_{broad}16\mu a/QE^{\infty}$, as a function of $a\kappa$. Solid curves are the numerical results for a uniform surface charge and a uniform edge charge. Dashed curves are the asymptotic approximations (57),(59) derived in Sec. III, and in the case of broadside motion for $a\kappa \gg 1$ the asymptote is given by (64) with the constant $C=0.226$.

tions for thick double layers (59), and for a thin double layer around a disk charged at its edge (57). These agree well with the numerical results. It was argued in Sec. III C that the broadside velocity of a uniformly charged disk would vary as

$$U_{broad} \sim C Q_{surf} E^{\infty}/2\mu\pi a^2\kappa, \tag{64}$$

and we may use the numerical results shown in Fig. 3 to establish $C=0.226$. This is smaller than the value $C=1$ predicted by Smoluchowski for edgewise motion (43).

Comparing Figs. 2 and 3 we see that as the double layer gets vanishingly thin ($a\kappa \to \infty$) the disk will move broadside since any edge charge leads to a finite broadside translational speed (57), while the other cases have velocities which vanish as $a\kappa$ increases.

Finally, we examine the ratio of the edge charge to surface charge Q_{edge}/Q_{surf} (<0) at which the electrophoretic velocity is zero. Results for both the transverse and edgewise motions of the disk are shown in Fig. 4. The principal conclusion to be drawn from this figure is that larger ratios of edge to surface charge are necessary to effect the same change in electrophoretic velocity for the case of edgewise motion as compared to broadside motion.

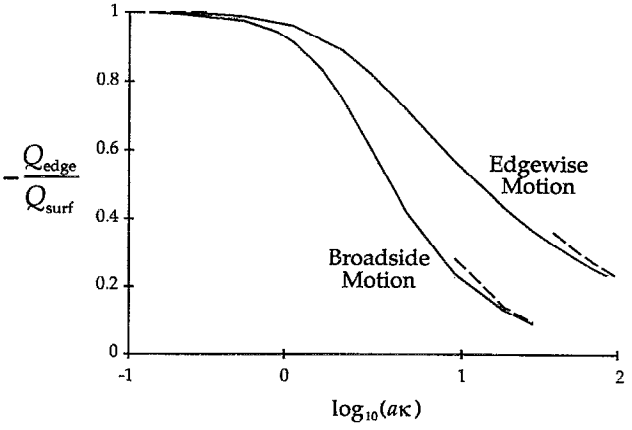

FIG. 4. The charge ratio $|Q_{edge}/Q_{surf}|$ at which the electrophoretic velocity is zero. The solid curves denote numerical results for edgewise and broadside motion and the dashed curves are based upon the asymptotic approximations developed in Sec. III.

V. DISCUSSION

The standard representation of a Na-montmorillonite particle is a flat plate with a uniform negative surface charge σ, typically[25,26] of order 0.1 C m^{-2}. In the absence of a Stern layer of adsorbed ions, linear Poisson–Boltzmann theory predicts a surface potential $\psi_0=\sigma/\epsilon\kappa$; the permittivity $\epsilon=\epsilon_0\epsilon_r$, where ϵ_0 is the permittivity of free space and ϵ_r is the relative permittivity of the fluid. Taking $\epsilon_r=80$ (water) and $\kappa^{-1}\simeq 10$ nm (1–1 electrolyte at 10^{-3} mol/l) we obtain $\psi_0=-1.4$ V, or $e\psi_0/kT=-55$. Nonlinear theory[27] predicts a nondimensional potential $e\psi_0/kT=2\sinh^{-1}(\sigma e/2\epsilon\kappa kT)=-8$, or $\psi_0=-200$ mV. Thus the linear theory of Sec. II would at first sight appear not to be appropriate for montmorillonite.

In practice, however, the surface charge σ is shielded by counterions which are to some extent bound to the surface. The degree of binding is ion-specific, as is observed in measurements both of electrophoretic velocities[28] and of the forces between particles.[26,29] Such ion binding is also predicted by Monte Carlo[30] and molecular dynamics[31] simulations of the clay–water interface. Measured zeta potentials usually have magnitudes in the range 0–100 mV. Full nonlinear computations of the electrophoretic velocity of spherical particles show[32] that linear theory is a good approximation up to nondimensional surface potentials of order 4. The linear analysis of Sec. II should therefore provide a reasonable approximation. When the Debye length κ^{-1} is small compared to the size of the particles (i.e., in the limit of a point particle), nonlinear computations indicate that the linear analysis holds to much higher potentials. This gives some reassurance that the high potentials associated with the edge charge q will not invalidate the linear analysis presented here.

The edge charge of a clay particle depends upon the pH, and electrophoretic velocities can increase by 50% or more[1,2] as the pH increases to values above 10. However, electrophoretic velocities which are independent of pH have also been reported,[33,34] and so have apparent zeta potentials which vary little with electrolyte concentration.[33] It has therefore been suggested[28,35] that a constant potential boundary condition might be more appropriate. These differences between the various experimental observations make it hard for us to compare theory against experiment. If the montmorillonite particles are large, the ratio of the edge charge $Q_{edge}=2\pi aq$ to the surface charge $Q_{surf}=2\pi a^2\sigma$ will decrease, thereby reducing the effect of the edge. Particle size therefore plays an important role.

The results presented in Secs. III and IV indicate that as the double layer becomes thinner, the edge charge gives a greater contribution to the electrophoretic velocity than the surface charge; the edge charge electrophoretic velocities are $O(a\kappa)^{1/2}$ larger for edgewise motion, and $O(a\kappa)$ larger for broadside motion. We may thus conclude that in the limit

$a\kappa \to \infty$, the disk will move broadside if the edge charge is nonzero. The electric field is singular at the edge of the particle, and interacts strongly with the edge charge. However, in practice, our analysis is no longer appropriate when the Debye length κ^{-1} becomes so small that the thickness of the clay platelet may no longer be neglected; for sufficiently thin double layers the analysis of Fair and Anderson[4] is more appropriate. They specified the zeta potential as a function of position over the surface of a spheroid, and assumed that the double layer was everywhere thin compared to the particle dimension.

Yoon and Kim[3] studied spheroids with a uniform zeta potential ψ_0, but with arbitrary double layer thickness. Our analysis is therefore similar to theirs in the limit in which an oblate spheroid becomes a disk. When the double layer is thin, there will be no difference between the condition of constant surface charge density σ adopted here, and that of constant zeta potential, except in a region $O(\kappa^{-1})$ around the edge of the particle. If Yoon and Kim had studied sufficiently thin double layers, their results, like those of Fair and Anderson, would ultimately agree with Smoluchowski (43). This limit is not reached in our own analysis of broadside motion of uniformly charged particles, as the double layer is never thin compared to the plate thickness, and hence $C \neq 1$ in (64). In this case, the charge at the center of the disk is shielded from the broadside electric field. It contributes little to the electrophoretic velocity, which depends upon the detailed distribution of ions and charge around the edge of the disk, where the field is high. Two limiting processes may be considered: that in which the double layer thickness around an oblate spheroid decreases to zero and that in which the spheroid approaches a flat disk. Clearly the two processes do not commute.

In the limit of a thick double layer ($a\kappa \ll 1$), the charge distribution at constant potential is (highly) nonuniform, and the results of Yoon and Kim differ from ours. In particular, at constant surface charge, we predict that the electrophoretic velocity decreases as $a\kappa$ increases, for both edgewise (60) and broadside motion (59). At constant potential, broadside velocities decrease (62), but edgewise velocities increase (63), as found numerically by Yoon and Kim.

ACKNOWLEDGMENTS

We thank Dr. S. K. Lucas for making available programs for integrating the Bessel function integrals and Dr. J. P. Tanzosh for helpful discussions regarding solutions to Stokes equations for the disk geometry. HAS thanks the National Science Foundation for support via a PYI Award (CTS-8957043).

[1]S. L. Swartzen-Allen and E. Matijević, "Colloid and surface properties of clay suspensions II. Electrophoresis and cation adsorption of montmorillonite," J. Colloid Interface Sci. **50**, 143 (1975).
[2]B. Rand, E. Pekenć, J. W. Goodwin, and R. W. Smith, "Investigation into the existence of edge-face coagulated structures in Na-Montmorillonite suspensions," J. Chem. Soc. Faraday Trans. I **76**, 225 (1980).
[3]B. J. Yoon and S. Kim, "Electrophoresis of spheroidal particles," J. Colloid Interface Sci. **128**, 275 (1989).
[4]M. C. Fair and J. L. Anderson, "Electrophoresis of nonuniformly charged ellipsoidal particles," J. Colloid Interface Sci. **127**, 388 (1989).
[5]D. C. Henry, "The cataphoresis of suspended particles," Proc. R. Soc. London Ser. A **133**, 106 (1931).
[6]J. D. Sherwood, "Electrophoresis of rods," J. Chem. Soc. Faraday Trans. II **78**, 1091 (1982).
[7]M. Teubner, "The motion of charged colloidal particles in electric fields," J. Chem. Phys. **76**, 5564 (1982).
[8]R. W. O'Brien and D. N. Ward, "The electrophoresis of a spheroid with a thin double layer," J. Colloid Interface Sci. **121**, 402 (1988).
[9]D. A. Saville, "Electrokinetic effects with small particles," Annu. Rev. Fluid Mech. **9**, 321 (1977).
[10]G. S. Manning, "Limiting laws and counterion condensation in polyelectrolyte solutions. I. Colligative properties," J. Chem. Phys. **51**, 924 (1969).
[11]M. Fixman, "The Poisson–Boltzmann equation and its application to polyelectrolytes," J. Chem. Phys. **70**, 4995 (1979).
[12]R. B. Secor and C. J. Radke, "Spillover of the diffuse double layer on Montmorillonite particles," J. Colloid Interface Sci. **103**, 237 (1985).
[13]F.-R. C. Chang and G. Sposito, "The electrical double layer of a disk-shaped clay mineral particle: effect of particle size," J. Colloid Interface Sci. **163**, 19 (1994).
[14]I. N. Sneddon, *The Use of Integral Transforms* (McGraw-Hill, New York, 1972), p. 350.
[15]I. S. Gradshteyn and I. M. Ryzhik, *Tables of Integrals, Series and Products* (Academic, New York, 1965).
[16]J. Happel and H. Brenner, *Low Reynolds Number Hydrodynamics* (Martinus Nijhoff, Amsterdam, The Netherlands, 1983).
[17]M. Ray, "Application of Bessel functions to the solution of problems of motion of a circular disk in viscous liquid," Philos. Mag. **21**, 546 (1936).
[18]S. C. Gupta, "Slow broad side motion of a flat plate in a viscous fluid," Z. Angew. Math. Phys. **8**, 257 (1957).
[19]A. M. J. Davis, "Some asymmetric Stokes flows that are structurally similar," Phys. Fluids A **5**, 2086 (1993).
[20]J. P. Tanzosh, "Integral equation formulations of the linearized Navier–Stokes equation: applications to particle motions in rotating viscous flows," Ph.D. dissertation, Harvard University, 1994.
[21]G. N. Watson, *Theory of Bessel Functions* (Cambridge University Press, Cambridge, 1945), p. 403.
[22]C. G. Phillips, "The steady, diffusion-limited current at a disk microelectrode with a first-order EC' reaction," J. Electroanal. Chem. **296**, 255 (1990).
[23]M. A. Bender and H. A. Stone, "An integral equation approach to the study of the steady state current at surface microelectrodes," J. Electroanal. Chem. **351**, 29 (1993).
[24]S. K. Lucas, "Evaluating infinite integrals involving products of Bessel functions of arbitrary order," J. Comput. Appl. Math. (in press, 1995).
[25]H. Van Olphen, *An Introduction to Clay Colloid Chemistry*, 2nd ed. (Wiley, New York, 1977).
[26]S. D. Lubetkin, S. R. Middleton, and R. H. Ottewill, "Some properties of clay–water dispersions," Philos. Trans. R. Soc. London Ser. A **311**, 353 (1984).
[27]W. B. Russel, D. A. Saville, and W. R. Schowalter, *Colloidal Dispersions* (Cambridge University Press, Cambridge, 1989).
[28]S. E. Miller and P. F. Low, "Characterization of the electrical double layer of montmorillonite," Langmuir **6**, 572 (1990).
[29]R. M. Pashley, "DLVO and hydration forces between Mica surfaces in Li^+, Na^+, K^+ and Cs^+ electrolyte solutions: a correlation of double-layer and hydration forces with surface cation exchange properties," J. Colloid Interface Sci. **83**, 531 (1981).
[30]N. T. Skipper, K. Refson, and J. D. C. McConnell, "Computer simulation of water in 2:1 clays," J. Chem. Phys. **94**, 7434 (1991).
[31]K. Refson, N. T. Skipper, and J. D. C. McConnell, "Molecular dynamics simulation of water mobility in smectites," in *Geochemistry of Clay–Pore Fluid Interactions*, edited by D. A. C. Manning, P. L. Hall, and C. R. Hughes (Chapman and Hall, London, 1993), pp. 62–77.
[32]R. W. O'Brien and L. R. White, "Electrophoretic mobility of a spherical colloidal particle," J. Chem. Soc. Faraday Trans. II **74**, 1607 (1978).
[33]I. C. Callaghan and R. H. Ottewill, "Interparticle forces in montmorillonite gels," Faraday Disc. Chem. Soc. **57**, 110 (1974).
[34]D. Heath and Th. F. Tadros, "Influence of pH, electrolyte and Poly(Vinyl Alcohol) addition on the rheological characteristics of aqueous dispersions of sodium montmorillonite," J. Colloid Interface Sci. **93**, 307 (1983).
[35]D. Y. C. Chan, R. M. Pashley, and J. P. Quirk, "Surface potentials derived from co-ion exclusion measurements on homoionic montmorillonite and illite," Clays Clay Miner. **32**, 131 (1984).